Mem. S.A.It. Vol. 75, 282

Memorie della

Structure of a slow CME in the low corona

A. Bemporad[1], G. Poletto[2] and J. Raymond[3]

[1] Astronomy & Space Science Dept., University of Firenze, L.go E. Fermi 2, 50125 Firenze, Italy, e-mail: bemporad@arcetri.astro.it
[2] INAF–Arcetri Astrophysical Observatory, L.go E. Fermi 5, 50125 Firenze, Italy
[3] Harvard–Smithsonian Center for Astrophysics, 60 Garden Street, Cambridge, MA 02138

Abstract. We report on UV and white light observations in the low corona of a Coronal Mass Ejection (CME) which occurred on January 31, 2000. From an analysis of SOHO/EIT, MDI and Yohkoh/SXT data we have been able to identify the Active Region (AR) source of the event, which is rapidly evolving, with a total area and total sunspot number increasing in time. The early evolution of this slow CME ($v \sim 500$ km s^{-1}) has been sampled by the SOHO/UVCS instrument at an heliocentric distance of 1.6 solar radii over a period of about 9 hours starting at about the time of the event initiation. This CME has been observed also with the Mauna Loa Mark IV coronagraph (which shows the white light corona between about 1.1 and 2.8 solar radii) over a time interval of 5 hours overlapping the UVCS observations period. These data have been used to estimate the electron density and average mass in different parts of the CME bubble. Next, from a comparison of the white light CME image with that reconstructed from the UV data, we identified in the UV line intensities the transit of the CME front, void and core through the UVCS slit. In order to reproduce the observed UV line intensities, in this work we qualitatively discuss the possible temperature variations across the CME bubble.

Key words. Sun: coronal mass ejections (CMEs) – Sun: UV radiation

1. Introduction

CMEs involve the catastrophic loss of equilibrium of a magnetic configuration with the release of the stored energy and a subsequent reconfiguration of the disrupted fields. Projected onto the plane of the sky they have typically a threee part structure consisting of 1) a bright leading edge (consequence of the plasma pile-up), 2) a dark void or cavity and 3) a bright core (identified as the rising flux rope). Over the last few years Lin & Forbes (2000), Lin, Raymond & van Ballegooijen (2004), Lin (2002) have thoroughly explored CME processes, from the CME initiation to its expansion through the solar corona and its manifestation at chromospheric levels. In these models, during the CME, the field is stretched outwards, due to the catastrophic loss of equilibrium of the flux rope: a current sheet forms in between the reconnecting loops and the lower tip of the bubble that grows around the flux rope as reconnection progresses outward.

In this work we analyze the early stages of a CME that occurred on January 31, 2000, for which we have data which cover the first hours of the CME evolution; our analysis is based on Mauna Loa, LASCO and UVCS observations.

Send offprint requests to: A. Bemporad

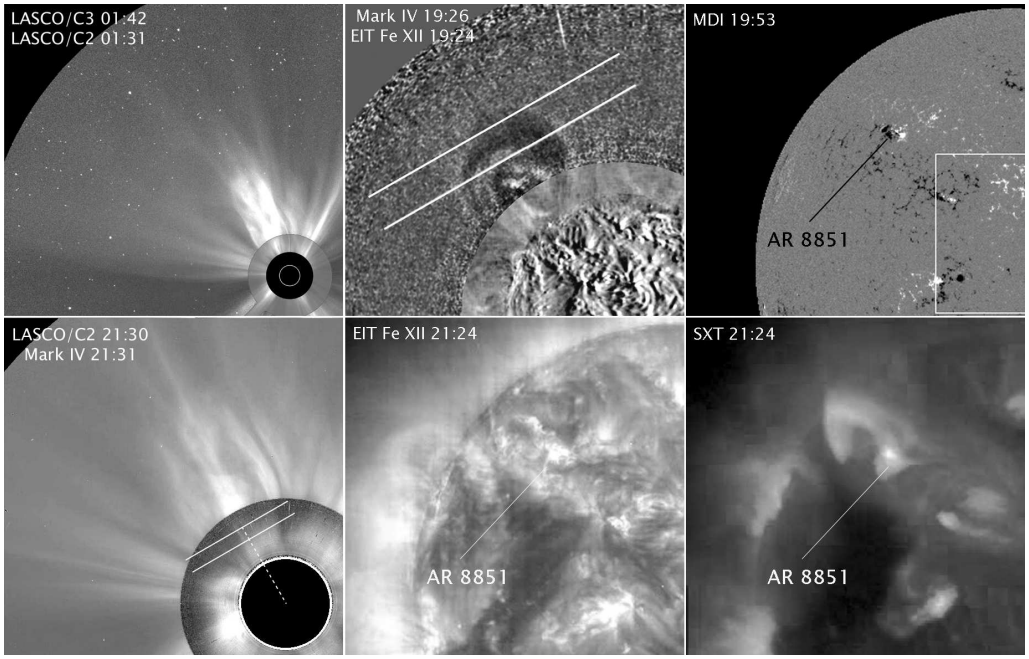

Fig. 1. Left: the January 31, 2000 CME as seen by the LASCO C3 (top, superimposed with a LASCO C2 image) and C2 (bottom, superimposed with a Mauna Loa Mark IV image) coronagraphs. Top middle: composite image obtained by superposing a difference Mauna Loa image (January 31, 19:23 – 19:32 UT) and an EIT Fe XII difference image (18:36 – 19:25 UT). Bottom middle: EIT Fe XII image showing the formation of a post-CME loop rooted in AR 8851. Bottom right: the same loop as seen by the Yohkoh SXT instrument. Top right: MDI image showing the positive (white) and negative (black) polarities of the magnetic field inside AR 8851. For future reference, the position of the slit of the UVCS spectrometer, centered at 1.6 and 1.9 solar radii at a latitude of 60°N, is given in the LASCO C2 and Mark IV panels.

In the first Section we discuss the identification of the CME source region on the disk, while in Sec. 2 we describe how we estimate from *pB* data the CME mass and density. In Sec. 3 we discuss the possible temperature variations across the CME and in Sec. 4 we present our conclusions.

2. The identification of the CME source region

On January 31, 2000 the LASCO C2 and C3 coronagraphs (Brueckner et al. 1995) aboard the SOHO satellite registered a slow CME which occurred in the North-East quadrant (centered at a latitude of 62°) and propagated in the outer corona with a radial speed of ~ 510 km/s at the heliocentric distance of about 8 $R_\odot$ (see Fig. 1) and a negligible acceleration[1]. As revealed by LASCO images, this CME has also a significant velocity component in the tangential direction (on the order of 80 km/s at the same distance) towards higher latitudes. As recently pointed out by Cremades & Bothmer (2004), a deviation towards higher latitudes with respect to the projected radial from the source region is a systematic phenomenon for CMEs occurring around the maximum of the solar activity cycle (as in our case); such deflections are probably due to the "fast solar wind flow from polar coronal holes that encompasses the CME's expansion at the higher latitudes" (Cremades & Bothmer 2004). This northward angular motion may affect the iden-

[1] See the LASCO CME catalog available on http://cdaw.gsfc.nasa.gov/CME_list/

tification on the disk of the CME source region. This is relevant to discuss possible relationships between the local AR field and the large scale ambient fields leading to the release of the flux rope, hence of the observed CME.

MDI data show (Fig. 1) on January 31, 2000 an active region (AR 8851) lying in the Northeast quadrant at a latitude of 27° and an eastern longitude of 42°; the radial from this AR projects onto the plane of the sky at a latitude of ∼ 54°N. White light images acquired in the low corona with the Mauna Loa Mark IV coronagraph show that at an heliocentric distance of 1.2 $R_\odot$ the CME is centered at about the same latitude (see Fig. 1). As a consequence, for simple geometrical reasons, we have a first indication that AR 8851 could be the CME source.

EIT images showing the activity in the low corona (see Fig. 1) seem to confirm this conclusion: difference EIT images in the Fe XII λ 195 Å spectral line show between 1 and ∼ 1.1 $R_\odot$ the formation of a nearly radial feature extending from the CME core (visible in the Mark IV difference images) to the disk limb. This feature, that can be identified as the post-CME current sheet, is aligned with the projected radial from AR 8851, as expected in the hypothesis that this is the CME source region (see Fig. 2). Moreover, starting from about 21:00 UT, a prominent loop (with a footpoint rooted in AR 8851) appears (Fig. 1), visible also in the soft Yohkoh SXT X-ray images. The presence of this high temperature ($T \approx 10^7$ K) loop may be an evidence of the post-CME reconnection which closes back the magnetic field opened by the CME leading to the formation of the current sheet (Fig. 2) and heats the plasma converting the energy stored in the magnetic field into kinetic and thermal energy. Hence, the appearance of this high temperature loop confirms that AR 8851 is the source of the CME.

Once the CME source region has been identified, an interesting issue we want to address is the analysis, starting from measurements of the photospheric magnetic field, of the possible effects of the interaction between the AR field and the external coronal field on the CME occurrence: however, the analysis of this problem is beyond the scope of this publication and will be illustrated in a future work. In the next Section we concentrate on the UVCS and Mark IV observations.

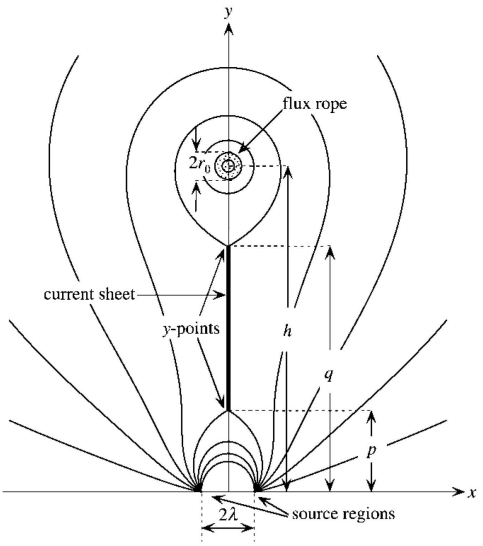

Fig. 2. Diagram of the Lin & Forbes (2000) CME/flux-rope configuration; this Figure can be compared with the observed configuration given in the middle top panel of Fig. 1.

3. Mark IV data: CME mass

The Mark IV K-Coronameter at the Mauna Loa Observatory measures the polarized brightness pB in the low corona (from ∼ 1.12 to ∼ 2.79 $R_\odot$) from 17:30 UT to 22:07 UT. Images from the Mauna Loa Mark IV Coronameter show at the time of the CME occurrence a complex system of rising loops which are seen later in the LASCO/C2 field of view. Difference images (Fig. 1, top middle panel) revealed a complex system of different loops surrounding a bright knot that we identify as the CME core. A comparison of the observed structure with that predicted by the Lin & Forbes (2000) CME model shows the two to be quite similar. The opening CME front, the following dark void and the CME core are visible; moreover, as revealed by a comparison with EIT Fe XII difference images, at this early stage of the event the current sheet

and the neutral "Y" point are already visible (see also Fig. 2). In the literature typically these structures are identified after the CME enters the LASCO/C2 field of view. To our knowledge, this is the first time that the 3 part structure of CMEs has been identified at such low coronal levels. As shown in Fig. 1, the UVCS slit is favorably located to observe the whole CME bubble; in particular from images at later times we expect to observe the transit of the core through the UVCS slit at about 20:00 UT.

The observed polarized brightness pB (usually normalized to the mean solar surface brightness $\bar{B}_\odot$) at an heliocentric distance of observation ρ is given by:

$$pB = \frac{\pi}{2}\sigma_T \bar{B}_\odot \int_{LOS} N_e \left[\frac{(1-u)A(r) + uB(r)}{1-u/3}\right]\frac{\rho^2}{r^2}dz$$

where σ_T is the total (i.e. integrated over all angles) Thomson cross section, r is the heliocentric distance, $z = \sqrt{r^2-\rho^2}$, $A(r)$ and $B(r)$ are geometrical functions (Altschuler & Perry 1972), u is the limb darkening coefficient in the visible wavelength of interest and the integral is extended along the line of sight (LOS). From the observed pB values it is possible to estimate the coronal electron density N_e with the advantage, with respect to the techniques which use EUV spectral lines, that the pB depends *solely* on the elecron density distribution N_e. However, in order to invert the above integral we need an a priori expression for the dependence of N_e on latitude and longitude (van de Hulst 1950). Assuming a profile for the electron density $N_e(r)$, it is possible to compute from the above equation a value for the expected $pB(\rho)_{exp}$ at a given heliocentric distance ρ of observation; the latter has to be compared with the observed value $pB(\rho)_{obs}$.

The above considerations led us to use the following method to evaluate the N_e in transient coronal structures. First, we assumed the coronal density to be spherically symmetric with density profile $N_e(r)_{GH}$ given by Guhathakurta & Holzer (1994). Then, analyzing the $pB(\rho)_{obs}$ values, we choose a region where no significant bright structures are visible and we evaluate the constant multiplier k of the $N_e(r)_{GH}$ profile we need to reproduce the observed pB. Finally, we assume that, in coronal regions where isolated structures (e.g. streamers and/or CMEs) are present, the electron density profile along the LOS is:

$$N_e(z) = k \cdot N_e(z)_{GH} \quad , \text{if } |z| > L/2$$
$$N_e(z) = k \cdot N_e(z)_{GH} + \bar{N}_e \quad , \text{if } |z| \le L/2$$

where $\bar{N}_e$ is the additional electron density that allows us (in a region centered on the plane of the sky with a length L (cm) along the LOS) to reproduce the observed pB. The length L is a free parameter that can be evaluated from the dimension projected onto the plane of the sky of the considered structure assuming an a priori geometry. This procedure has been applied pixel by pixel along the position of the UVCS slit to the region occupied by the CME, throughout the time interval covered by our observations.

In this work the background pB has been reproduced by multiplying the Guhathakurta & Holzer (1994) density profile by a factor $k = 6$, while the CME density has been derived by assuming an increased density $\bar{N}_e$ over an extension along the LOS $L = 1\ R_\odot$ centered on the plane of the sky. This assumption has been suggested by the average dimension projected onto the plane of the sky of the CME bubble (see Figure 1), which supposedly moves on that plane (because lines do not appear to be Doppler shifted). From this procedure we derive that the additional densities $\bar{N}_e$ needed to reproduce the observed pB in the CME front, void and core at the CME axis are, respectively, $2.6 \cdot 10^6$, $2.0 \cdot 10^6$ and $3.6 \cdot 10^6$ cm^{-3}, while the average background density $< N_e > = \int_{-L/2}^{+L/2} N_e(z)_{GH}\, dz/L$ is about $7.6 \cdot 10^6$ cm^{-3}.

Once the densities have been derived from the pB data, the mass of the different parts of the CME can be estimated by assuming that the additional electron density $\bar{N}_e$ is representative of the CME plasma. Because the CME 3D geometry is unknown, the derived values will give only the order of magnitude of the real CME mass and depend on the assumed geometry. In this work this mass has been computed by assuming for the CME geometry either a) a high density spherical blob of plasma with

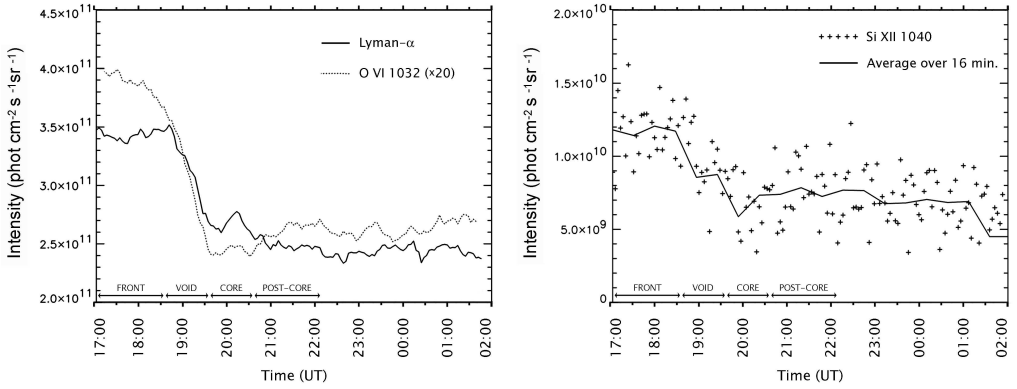

Fig. 3. Left: the Lyα λ 1216 Å and O VI λ 1032 Å intensity evolution at 1.6 $R_\odot$ averaged over 10° around a latitude of 50°N (hence at the CME axis). Note that both spectral lines show an intensity decrease (which correspond to the transit of the CME void), but only the Lyα line has a significant emission at the CME core (around ~ 20:00 UT); this is interpreted as a combination of temperature and Doppler dimming effects (see later). Right: the time evolution of the Si XII λ 1040 Å line (plus signs) and the average over 16 minutes (solid line) showing possibly a minimum at the time of the CME core transit.

radius r_0 (see Fig. 2) surrounded by two hemispherical shells representing the CME void and front, or b) a cylindrical core with base surface πr_0^2 extending over a depth of one solar radii along the LOS surrounded by two semicilindrical sheaths. Typical values for r_0 (~ 0.1 $R_\odot$) and for the dimensions of the other CME substructures have been derived from the Mark IV observations (see Fig. 1). Hence, with the densities given above, the total CME mass we estimate is on the order of $6 - 8 \cdot 10^{14}$g depending on the adopted geometry. This mass resides mostly in the CME front surrounding the core, while the mass of the core is less than 10% of the total CME mass.

4. UVCS data: CME temperatures

The UVCS (Kohl et al. 1995) observations started on January 31, 2000 at 17:05 UT and ended on February first at 02:00 UT. The UVCS slit was centered at a Northern latitude of 60° in the East quadrant (see Fig. 1) and two observation heights have been used, 1.6 and 1.9 $R_\odot$: the instrument took alternatively 12 exposures at 1.6 and 3 exposures at 1.9 $R_\odot$ (with an exposure time of 120 s), hence we have nearly "simultaneous" observations of the same event at two different altitudes. The slit width was 50 μm: data were acquired with a spatial binning of 6 pixels (i.e. a spatial resolution of 42") and a spectral binning of 1–3 pixels depending on the selected wavelength interval. The most intense spectral lines included in the selected spectral ranges are the hydrogen Lyman-α λ 1216 Å the O VI $\lambda\lambda$ 1032–1037 Å doublet and the Si XII λ 1040 Å (second order). In this work we report only results fron an analysis of data acquired at 1.6 $R_\odot$, because the analysis of data at 1.9 $R_\odot$ is still in progress.

The evolution with time of the observed Lyα, O VI and Si XII line intensities (averaged over the latitude of the core transit) are given in Fig. 3; in this Figure, taking advantage of the white light observations where different CME features are clearly visible, we identified the transit through the UVCS slit of the CME front, void and core (as indicated on the x axis of Figure 3). This Figure shows that the core structure in the Lyα line (intensity bump at about 20:00 UT) is only ~ 10% higher than the background emission, while is hardly identifiable in the O VI line and possibly corresponds to an intensity minimum in the Si XII line. On the contrary, the observed pB (as well as densities we derived) maximizes at the CME core (see Fig. 1), hence we may expect an higher emission from the core also in the UV line.

We briefly remind the reader that these three spectral lines are related to different atomic processes: the Lyα and Si XII line emissions are due, respectively, only to the absorption of photons from the background radiation (radiative excitation) and the to atomic collisions with thermal electrons (collisional excitation), while both contributions can be important for the O VI line. The main difference is that (in first approximation) the radiative and collisional components are proportional, respectively, to N_e and N_e^2. Moreover, the radiative component of the O VI and Lyα lines can be Doppler dimmed, but the O VI collisional component and the intensity of the Si XII line can be reduced (despite an increasing in electron density) only by temperature effects. In particular, because the O VI and Si XII emissivities (given by the CHIANTI spectral code) peak, respectively, at temperatures of $\log T = 5.5$ and $\log T = 6.3$, a decrease of the collisional component of both lines can be justified only by a temperature increase above $\log T = 6.3$. From this qualitative analysis we may conclude that, in order to reproduce the observed line intensities (Fig. 3) the core region has to be denser and hotter than the surrounding plasma. A more quantitative analysis requires a knowledge of the plasma outflow speed of different CME structures (that we can derive from *pB* observations) in order to evaluate the amount of Doppler dimming for O VI and Lyα lines; this will be done in the near future.

5. Discussion and conclusions

In this work we studied the early evolution of a CME which occurred on January 31, 2000, with the aim of inferring its structure and estimate physical parameters in different parts of a CME in the early stage of its development. From white light and UV data it has been possible to identify, less than one hour after its initiation, the typical three parts of a CME (front, void and core). From the *pB* data we derived the electron densities in these structures and (by assuming some simple CME geometries) the CME mass. The total CME mass we compute ($6 - 8 \cdot 10^{14}$ g) is about 1/3 of its total mass, derived at higher levels from LASCO/C3 images; however, the mass of a CME increases with increasing heliocentric distances (Lin, Raymond & van Ballegooijen 2004), because of the progressive reconnection of new fieldlines around the CME bubble and it is possible that the mass value we derive is representative only of the mass of the CME in the early phase of its development.

From a qualitative analysis of the spectral line intensity evolution observed by UVCS, we conclude that (taking into account the density variations derived from *pB* data) the faint or absent UV emission at the CME core can be explained only by assuming an higher plasma temperature in this region. This temperature increase is confirmed also by the detection of an O VI λ 1032 Å line broadening at the CME void and core which corresponds to an oxygen kinetic temperature about 25% larger in these regions. In the near future we plan to evaluate quantitatively the plasma heating needed to reproduce the line intensities and line broadening, possibly taking advantage also of UVCS data acquired at 1.9 $R_\odot$, so far not analyzed.

Acknowledgements. This work initiated during a visit of A.B. to the Harvard-Smithsonian Center for Astrophysics whose hospitality and support is gratefully acknowledged. A.B. and G.P. work has been partially supported by COFIN 2003029124_003. SOHO is a mission of international cooperation between ESA and NASA.

References

Altschuler, M.D., & Perry, R.M. 1972, SP, 23, 410

Brueckner, G.E. et al. 1995, SP, 162, 357

Cremades, H., & Bothmer, V. 2004, A&A, 422, 307

Guhathakurta, M., & Holzer, T.E. 1994, ApJ, 426, 782

Kohl, J.L. et al. 1995, SP, 162, 313

Lin, J. 2002, Chin. J. Astron. Astrophys., 2, 539

Lin, J. & Forbes, T.G. 2000, J. Geophys. Res., 105, 2375

Lin, J., Raymond, J.C., & van Ballegooijen, A.A. 2004, ApJ, 602, 422

van de Hulst, H.C. 1950, Bull. Astron. Inst. Netherlands, 11, 135